



Reference Module in Earth Systems and Environmental
Sciences
2020

Geoneutrinos: Seeing the Earth With Particle Physics

Ondřej Šrámek

Show more



Outline



Share



Cite

<https://doi.org/10.1016/B978-0-08-102908-4.00161-2>

[Get rights and content](#)

Abstract

Geoneutrinos are electron **neutrinos** and **antineutrinos** emitted in **radioactive decays** of **radionuclides** naturally occurring in the Earth. Thanks to experimental advances in fundamental neutrino research, geoneutrinos from ^{232}Th and ^{238}U decay chains have now been independently measured by two experiments, and more measurements are expected in the coming years. The flux of geoneutrinos at a detector location scales with the inverse of the squared distance to the **emitter**, and is thus a nontrivial function of the abundance and spatial distribution of the radionuclides in the Earth interior. Geoneutrino measurements provide a particle physics tool to investigate the inaccessible Earth, namely to place limits on the amount of Th and U, therefore radiogenic power available in various domains inside the Earth. A movable ocean-bottom geoneutrino detector, technology to detect the direction of the incoming geoneutrino, and method to detect geoneutrinos from ^{40}K decay all remain exciting goals in neutrino geoscience.

Keywords

Antineutrino; Borexino; Geoneutrino; Inverse beta decay; JUNO; KamLAND; Neutrino; Potassium; Radiogenic heat; SNO+; Thorium; Uranium

Recommended articles

Citing articles (0)



Ondřej Šrámek researches in geophysics, teaches physics and mathematics, plays double bass, and rides a pink bike in Praha, Czech Republic (<http://geo.mff.cuni.cz/~sramek>).

Copyright © 2020 Elsevier Inc. All rights reserved.



About ScienceDirect

Remote access

Shopping cart

Advertise

Contact and support

Terms and conditions

Privacy policy

We use cookies to help provide and enhance our service and tailor content and ads. By continuing you agree to the **use of cookies**.

Copyright © 2020 Elsevier B.V. or its licensors or contributors. ScienceDirect® is a registered trademark of Elsevier B.V.

ScienceDirect® is a registered trademark of Elsevier B.V.

Geoneutrinos: Seeing the Earth With Particle Physics

Ondřej Šrámek, Department of Geophysics, Faculty of Mathematics and Physics, Charles University, Prague, Czech Republic

© 2020 Elsevier Inc. All rights reserved.

Neutrinos and Geoneutrinos	2
Radioactive Decay and Radiogenic Heat	2
Geoneutrino Emission	2
Antineutrino Detection	5
Geoneutrino Measurements	6
Advancing Geoscience with Geoneutrinos	8
Prospects in Geoneutrino Research	9
Acknowledgment	10
References	10

Glossary

ANDES Agua Negra Deep Experiment Site, a proposed underground physics laboratory to be built in the Agua Negra tunnel connecting Chile and Argentina below the Andes mountains.

BLVST Baksan Large Volume Scintillation Telescope, a neutrino experiment proposed at the Baksan Neutrino Observatory (BNO) located in the Baksan River gorge in the Caucasus mountains in Russia.

Borexino A neutrino experiment located at the Laboratori Nazionali del Gran Sasso (LNGS) in Italy, taking data since December 2007.

eV, keV, MeV The energy unit of electronvolt and derived units (kiloelectronvolt, megaelectronvolt), commonly used in nuclear and particle physics. Conversion to SI units is $1 \text{ MeV} \approx 1.602 \times 10^{-13} \text{ J}$.

Geoneutrino Electron neutrino or antineutrino emitted in radioactive β -decay of a radionuclide naturally occurring in the Earth.

Inverse beta decay (IBD) The reaction $\bar{\nu}_e + p \rightarrow e^+ + n$ (antineutrino + proton \rightarrow positron + neutron), which is the current leading method to detect geoneutrinos and other antineutrinos in the few-MeV energy range.

JNE Jinping Neutrino Experiment, proposed at the China Jinping underground Laboratory (CJPL) in Sichuan province, China.

JUNO Jiangmen Underground Neutrino Observatory, a neutrino experiment being built in Guangdong province, China.

KamLAND Kamioka Liquid-scintillator Anti-Neutrino Detector, a neutrino experiment taking data since January 2002 at the Kamioka Observatory near Hida in Gifu prefecture, Japan.

Neutrino, antineutrino Subatomic particles, leptons with no electric charge, that interact only via the weak force (related to nuclear decay) and gravity.

SNO+ A neutrino experiment, located at the site of the previous SNO (Sudbury Neutrino Observatory) experiment at SNOLAB in Ontario, Canada.

Summary

The Earth naturally contains K, Th, U whose radioactive nuclides upon decay

- produce radiogenic heat that powers Earth's dynamics,
- emit *GEONEUTRINOS* (electron antineutrinos and neutrinos).

The higher energy ($>1.8 \text{ MeV}$) antineutrinos from ^{232}Th and ^{238}U decay chains have been measured via the *INVERSE BETA DECAY* mechanism ($\bar{\nu}_e + p \rightarrow e^+ + n$) by two kiloton-scale liquid scintillator antineutrino detectors (KamLAND, Borexino) constructed in underground physics laboratories in Japan and Italy.

Two other detectors will measure geoneutrinos in the next decade (SNO+, JUNO), and more are planned (JNE, ANDES, BLVST).

Comparing measurements with Earth model predictions places limits on Th and U abundances in the Earth.

Proposed measurement with an ocean-bottom detector (OBD) can tightly constrain the mantle radiogenic power; multisite OBD measurement could interrogate potential 3D structure of the mantle.

Geoneutrino measurement of Earth's Th/U ratio is, in principle, possible. Work is in progress toward measuring geoneutrinos from ^{40}K decay, which would constrain Earth's K/U ratio.

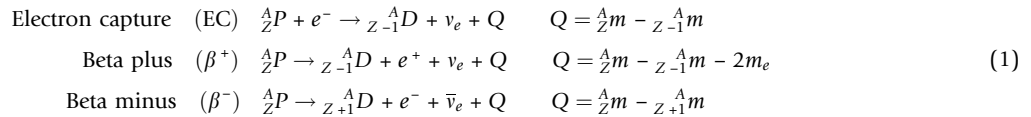
Neutrinos and Geoneutrinos

Neutrinos and their antimatter counterpart antineutrinos are subatomic particles, common around us and in the universe, where they are the second most abundant of the known particles (after photons). These leptons (i.e., fermions that do not interact via strong interactions) with no electric charge (and which are associated with their charged counterparts electron, muon, and tau) now assume a solid place in the Standard Model of particle physics—even stimulate and require an updated particle physics model!—but the story of their becoming is a great tale in the history of science (Close, 2010). Sources of neutrinos and antineutrinos are diverse and many, and include nuclear reactions and thermal processes in stars, supernova explosions, cosmic ray interactions with Earth’s atmosphere, processes happening immediately after the Big Bang (i.e., cosmic neutrino background and Big Bang neutrinos), as well as man-made nuclear reactors (Vitagliano et al., 2019). Those neutrinos and antineutrinos that are created in spontaneous nuclear β -decays of radionuclides naturally occurring in terrestrial rocks, we call *GEONEUTRINOS*. They are electron (and not muon nor tau) neutrinos (ν_e) created in electron capture (EC) and β^+ decays, and electron antineutrinos ($\bar{\nu}_e$) created in β^- decays.

Of the four fundamental interactions in physics, neutrinos (and antineutrinos) interact via the *WEAK INTERACTION* (related to nuclear decays). Given their nonzero mass, an exciting finding obtained in fundamental neutrino physics research of the past few decades and related to the rather mind-boggling manifestation of neutrino oscillation, neutrinos, in principle, also interact via the gravitational interaction. However, given their tiny mass (at most about 10^{-6} times the mass of the electron; <http://pdg.lbl.gov>), in most settings—and definitely in our discussion of geoneutrinos—gravitational interaction can be safely neglected. Neutrinos do not interact via the strong interaction nor the electromagnetic interaction.

Radioactive Decay and Radiogenic Heat

The radioactive decay reactions for a nucleus of the parent nuclide ${}^A_Z P$ with a proton number Z and a mass number A , decaying into a daughter nuclide D , can be noted as follows:

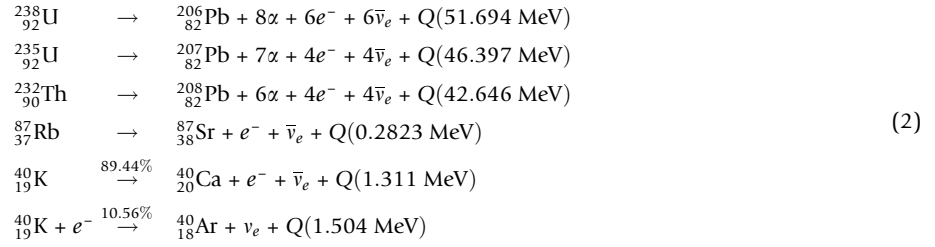


where e^- is the electron, e^+ is the positron, Q denotes the energy released in the decay (in convenient energy units such as MeV), ${}^A_Z m$ is the mass of the corresponding neutral atom (in units of energy, which exploits the famous Einstein’s equation $E = mc^2$), and m_e is the mass of an electron. In writing the expression for the decay energies Q , the usual and justified assumption of neglecting the binding energy between individual electron pairs has been made (e.g., Magill and Galy, 2005). The atomic masses are tabulated and easily accessible (e.g., <http://www.nist.gov/pml/data/comp.cfm>, and references therein).

Upon a β -decay of a radionuclide inside the Earth, part of this decay energy Q is carried by the geoneutrino as its kinetic energy. Due to the negligibly small interaction cross section with matter (rocks in the Earth) at the relevant neutrino energy scale of the order of 1 MeV, this energy escapes the Earth with the geoneutrino. The remaining part of Q is the kinetic energy of the electron or positron and possibly the de-excitation energy (in the case of decay to an excited energy level of the daughter nuclide). This part of Q is eventually released in the Earth in the form of *RADIOGENIC HEAT*. In the case of β^+ decay, an additional contribution to radiogenic heat, not accounted for in Q , comes from the annihilation of the resulting positron with an ambient electron. In the case of decay to an excited state of the daughter nucleus, part of Q is subsequently released in the form of γ -radiation and contributes to radiogenic heat. Of course, β radioactivity is not the only one contributing heat: In α decays (especially those in decay networks of Th and U nuclides; Eq. 2), all of the released energy remains in the Earth, being deposited by the slowing α particle, and released as γ radiation in decays to an excited level. *This provides the link between radioactive decays, geoneutrinos, and the radiogenic heat as an internal energy source that powers the large-scale dynamics of the Earth.* The geoneutrino flux, that is, the number of geoneutrinos that pass through a unit area per unit time, can be inferred from experimental geoneutrino detection at the detector sites, and this information can then be harvested to constrain our knowledge of select radionuclides’ distribution in the Earth.

Geoneutrino Emission

The rate of geoneutrino emission in the Earth (or any domain within the Earth) scales with the abundance of radionuclides. Various estimates of Earth’s composition proposed by geochemists, despite some important differences in concentrations of some elements stemming from different approaches, all identify the following major contributors to the Earth’s geoneutrino production: radionuclides of uranium (${}^{238}\text{U}$, and ${}^{235}\text{U}$ usually tags along because of its more important relative contribution to heat production), thorium (${}^{232}\text{Th}$), potassium (${}^{40}\text{K}$), and rubidium (${}^{87}\text{Rb}$). The three actinides decay along decay chains, which contain α - and β -decays.



Combining the relevant radioactive decay input quantities, listed in Table 1, one can evaluate the specific geoneutrino luminosity, per unit mass of pure element of its natural isotopic composition. This quantity is independent of rock composition. Then, given an average composition as mass fractions of elements, one gets the specific geoneutrino luminosity per unit mass of rock. Multiplying with the mass of the domain of interest, one gets the total geoneutrino luminosity. A similar exercise can be done for radiogenic heat production. These quantities are listed in Table 1. The evaluation is performed for a Bulk Earth compositional model (see Table 1 caption for details and references). Fig. 1 shows the relative contributions of the geoneutrino luminosity and of radiogenic power for such compositional model. The relative magnitudes of the contributions scale with the Th/U, K/U, and Rb/U ratios, where the largest uncertainty comes with the volatile K.

Given a model of the spatial distribution of geoneutrino emitters in the Earth (abundance A as mass fraction of elements), one can produce a prediction map of geoneutrino flux spectrum $d\phi/dE$ (# of geoneutrinos passing per unit area per unit of energy of the (anti)neutrino) at the Earth's surface by integrating over the planet's volume (\oplus) with matter density ρ ,

Table 1 Geoneutrino-emitting and heat-producing nuclides in present-day Earth.

	${}^{238}\text{U}$	${}^{235}\text{U}$	${}^{232}\text{Th}$	${}^{40}\text{K}$	${}^{87}\text{Rb}$
Decay mode	α, β^- chain	α, β^- chain	α, β^- chain	β^- or ϵ	β^-
Natural mole frac. X	0.992740	0.0072049	1.0000	1.167×10^{-4}	0.2783
Nuclide mass (g mol $^{-1}$)	238.0508	235.0439	232.0381	39.9640	86.9092
Std. atom. Weight M (g mol $^{-1}$)	238.0289	238.0289	232.038	39.098	85.468
Half-life $t_{1/2}$ (10 9 a)	4.4683 (96)	0.70348 (20)	14.1 (1)	1.262 (2)	49.61 (16)
Decay constant λ (10 $^{-18}$ s $^{-1}$)	4.916	31.223	1.56	17.40	0.4428
$n_{\bar{\nu}_e}$ (antineutrinos per decay)	6	4	4	0.8944	1
n_{ν_e} (neutrinos per decay)	0	0	0	0.1056	0
Q (MeV)	51.694	46.397	42.646	1.3313	0.2823
Q (pJ)	8.2823	7.4335	6.8326	0.2133	0.0452
Q_{ν} (MeV)	4.050	2.020	2.230	0.655	0.200
Q_{ν} (pJ)	0.649	0.324	0.357	0.105	0.032
Q_h (MeV)	47.6	44.4	40.4	0.676	0.082
Q_h (pJ)	7.633	7.110	6.475	0.108	0.013
l_{ν_e} (kg-element $^{-1}$ s $^{-1}$)	0	0	0	0	0
$l_{\bar{\nu}_e}$ (kg-element $^{-1}$ s $^{-1}$)	7.636×10^7		1.617×10^7	2.797×10^4	8.682×10^5
h ($\mu\text{W kg-element}^{-1}$)	98.293		26.180	0.003387	0.01136
Element mass frac. A (kg kg $^{-1}$)	2.00×10^{-8}	2.00×10^{-8}	7.54×10^{-8}	2.80×10^{-4}	6.00×10^{-7}
Nuclide mass frac. (kg kg $^{-1}$)	1.99×10^{-8}	0.0144×10^{-8}	7.54×10^{-8}	3.276×10^{-8}	1.67×10^{-7}
L_{ν_e} (s $^{-1}$)	0	0	0	3.74×10^{24}	0
% contribution to total L_{ν_e}	0	0	0	99.96%	0
$L_{\bar{\nu}_e}$ (s $^{-1}$)	5.99×10^{24}	1.84×10^{23}	4.93×10^{24}	3.17×10^{25}	2.11×10^{24}
% contribution to total $L_{\bar{\nu}_e}$	13.2%	0.41%	10.9%	69.8%	4.6%
H (W)	7.62×10^{12}	3.27×10^{11}	7.98×10^{12}	3.83×10^{12}	2.77×10^{10}
% contribution to total H	38.4%	1.6%	40.2%	19.3%	0.14%

Q , decay energy (energy released per decay of one atom); Q_{ν} , energy carried away by the electron neutrino or antineutrino per decay; Q_h , energy remaining to provide radiogenic heating per decay; $l_{\nu_e}, l_{\bar{\nu}_e}$, specific (anti)neutrino luminosities of pure element (# particles per kg-element per second); h , specific radiogenic heat of pure element (power per kg-element); Element mass frac., element abundance in silicate Earth (kg-element per kg-rock); Nuclide mass frac., nuclide abundance in silicate Earth (kg-nuclide per kg-rock); $L_{\nu_e}, L_{\bar{\nu}_e}$, (anti)neutrino luminosity of the Earth; H , radiogenic heat production in the Earth.

The Earth compositional model assumes negligible amounts of the listed radionuclides in the core, and a Silicate Earth model of McDonough and Sun (1995), with an update on K/U of Arevalo et al. (2009), and an update on Th/U of Wipperfurth et al. (2018). See McDonough et al. (2020) for detailed description. Total natural antineutrino luminosity is $L_{\bar{\nu}_e}^{\text{tot}} = 3.74 \times 10^{24} \text{ s}^{-1}$ and the remaining 0.04% comes from ${}^{138}\text{La}$ decay. Total neutrino luminosity is $L_{\nu_e}^{\text{tot}} = 4.54 \times 10^{25} \text{ s}^{-1}$ and the remainder comes primarily from ${}^{187}\text{Re}$ (1.06%) and ${}^{176}\text{Lu}$ (0.03%). The total geoneutrino luminosity ($\nu_e + \bar{\nu}_e$) is then $L_{\text{geov}}^{\text{tot}} = 4.91 \times 10^{25} \text{ s}^{-1}$. The total radiogenic heat production is $H = 19.86 \text{ TW}$, where the remainder comes from ${}^{147}\text{Sm}$ (0.38%).

Adapted from McDonough WF, Šrámek O, and Wipperfurth SA (2020) Radiogenic power and geoneutrino luminosity of the Earth and other terrestrial bodies through time. *Geochemistry, Geophysics, Geosystems*, e2019GC008865. <https://doi.org/10.1029/2019GC008865>. arXiv:1912.04655; <https://doi.org/10.1002/essoar.10501374.1>.

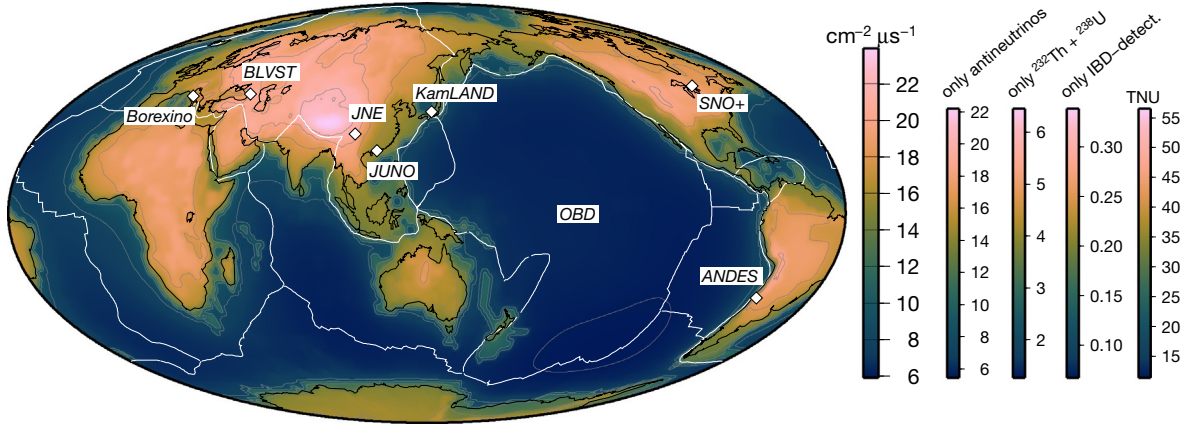


Fig. 3 Prediction of geoneutrino flux at Earth’s surface. Calculation includes geoneutrinos (antineutrinos and neutrinos) emitted by all natural radionuclides. Additional scale bars to the right indicate how the value range would change if one plotted only antineutrinos ($\bar{\nu}_e$), only $\bar{\nu}_e$ from ^{232}Th and ^{238}U , only the IBD-detectable $\bar{\nu}_e$ from these two nuclides, and the corresponding TNU values—while the map pattern remains nearly identical (IBD and TNU explained in section *Antineutrino detection*). Adapted from Šrámek O, McDonough WF, Kite ES, Lekić V, Dye ST, and Zhong S (2013) Geophysical and geochemical constraints on geoneutrino fluxes from Earth’s mantle. *Earth and Planetary Science Letters* 361: 356–366. <https://doi.org/10.1016/j.epsl.2012.11.001>. arXiv:1207.0853.

Antineutrino Detection

Following the first detection of electron antineutrinos emitted by the nuclear reactor core of the Savannah River Plant in South Carolina, USA (Cowan et al., 1956, Nobel Prize 1995), essential questions in fundamental neutrino research required focused experimental efforts, which continue to be one of the flagship themes of basic physics research at present. Great progress has been made toward understanding the fundamental nature and properties of neutrinos, notably rewarded by several Nobel Prizes (1988, 1995, 2002, 2015) and the 2016 Breakthrough Prize in fundamental physics. Reactor neutrino experiments are built close to man-made nuclear reactors, which provide a high flux of electron antineutrinos, emitted in decays of fission products of the nuclear fuel burning. The energy spectrum of these reactor neutrinos with energies on the order of a few MeV overlaps with the geoneutrino spectrum and extends beyond up to ~8 MeV (Fig. 2).

The leading method to detect these few-MeV antineutrinos is the *inverse beta decay* (IBD) reaction, where the antineutrino interacts with a proton (p), leading to production of a neutron (n) and a positron (e^+) (Eq. 4). This reaction has an energy threshold of 1.806 MeV (as $n + e^+$ are heavier than $\bar{\nu}_e + p$), meaning that only antineutrinos with kinetic energy $E \geq 1.806$ MeV can participate. A prompt signal comes from the positron’s kinetic energy losses through ionization and subsequent positron–electron annihilation in the detector medium (Eq. 5). A delayed signal follows when the neutron is captured by a proton in the medium to form a deuteron (Eq. 6) (in some experiments, the neutron is captured by a heavier nucleus).

$$\bar{\nu}_e + p \rightarrow e^+ + n \quad \text{Inverse beta decay} \quad (4)$$

$$e^+ + e^- \rightarrow \gamma + \gamma \quad \text{Prompt signal} \quad (5)$$

$$n + p \rightarrow d + \gamma \quad \text{Delayed signal} \quad (6)$$

The spatial and temporal coincidence of the double-flash signal (prompt followed by delayed, Fig. 4) provides a unique tag of the antineutrino interaction and helps suppress unwanted, non-antineutrino background. The non-antineutrino background includes

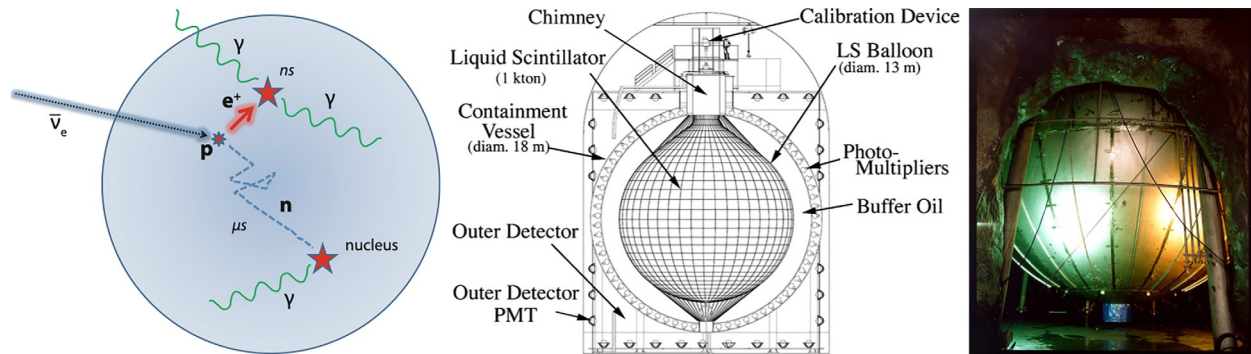


Fig. 4 Schematic of IBD (inverse beta decay) interaction (left), and schematic (middle) and photograph (right) of the KamLAND detector; the diameter of the main balloon is ~13 m. Adapted from Šrámek O, McDonough WF and Learned JG (2012) Geoneutrinos. *Advances in High Energy Physics*, Special Issue on Neutrino Physics, Article ID 235686. <https://doi.org/10.1155/2012/235686>; en.wikipedia.org, and www.awa.tohoku.ac.jp/kamlande.

cosmogenic background (in particular fast neutrons, and decays of the spallation nuclides ${}^9\text{Li}$ and ${}^8\text{He}$), possible (α, n) reactions initiated by α particles due to impurities in the materials of the detector, accidental double-flash IBD-like coincidences, and atmospheric neutrinos (e.g., Gando et al., 2013; Agostini et al., 2020). Reactor antineutrinos from man-made nuclear reactors constitute the antineutrino background from the perspective of geoneutrino detection (while typically being the primary wanted signal in the research agenda of reactor experiments such as KamLAND and JUNO) (Baltoncini et al., 2015).

The interaction cross section (essentially, the probability of the interaction, with physical units of surface area) of the IBD reaction, σ_{IBD} , increases with neutrino energy and starts at the IBD threshold energy of 1.806 MeV (Vogel and Beacom, 1999; Dye, 2012) (Fig. 2). Multiplication of the production spectra with the IBD cross section yields the IBD interaction spectrum of geoneutrinos (Fig. 2). It clearly shows that only the highest energy antineutrinos from ${}^{232}\text{Th}$ and ${}^{238}\text{U}$ decay chains can be detected via the IBD interaction. These antineutrinos originate in the ${}^{228}\text{Ac}$ and ${}^{212}\text{Bi}$ β^- decays of the ${}^{232}\text{Th}$ chain, and in ${}^{234}\text{Pa}$ and ${}^{214}\text{Bi}$ decays of the ${}^{238}\text{U}$ chain (Fiorentini et al., 2007).

It is perhaps more straightforward to multiply the IBD cross section σ_{IBD} with the antineutrino flux $d\phi/dE$ (Eq. 3) and integrate over the relevant energy range (1.8–3.3 MeV),

$$\int \frac{d\phi(\vec{r}, E)}{dE} \sigma_{\text{IBD}}(E) dE, \quad (7)$$

which yields the IBD event rate, that is, the number of interactions per second per proton. It is of the order of 10^{-38} event s^{-1} proton $^{-1}$ at Earth's surface. A more convenient, experiment-scale unit was devised to quantify the geoneutrino signal: the terrestrial neutrino unit, or TNU, which is the number of IBD events on 10^{32} target protons (order of magnitude of current detectors) per 1 year, assuming fully efficient detection. The TNU signal is thus obtained by multiplying the expression in Eq. (7) by $10^{32} \times 31,556,925.445 \approx 3.16 \times 10^{39}$ (the second factor being the number of seconds in a year; Holden et al., 2011). The presence of geoneutrinos can therefore be equivalently quantified as IBD event rate (event s^{-1} proton $^{-1}$), or in TNU (event rate rescaled to convenient values, see Fig. 3), or as flux ($\bar{\nu}_e \text{ cm}^{-2} \mu\text{s}^{-1}$). All these units are used in the literature, both for reporting the experimental measurements and for calculating geoneutrino signal predictions based on Earth models. Additionally, sometimes the event rate, in units of recorded events per year, is reported for a particular detector; unlike the normalized TNU value, it depends on the specifics of the detector, such as its size and the efficiency of registering the IBD interactions.

In order to detect antineutrino events, one needs to assemble a large enough number of free protons (typically order of 10^{32}), expose them to antineutrino flux for sufficient time (order of years)—thus achieving sufficient *EXPOSURE* (measured in units of proton \times years)—and be able to register IBD interactions. Neutrino detectors are essentially huge (kiloton scale), ultra radiopure tanks of liquid scintillator, surrounded by photomultiplier tubes (or PMTs, ultra-sensitive photon detectors), the whole assembly placed underground to shield the detector from unwanted effects of cosmic rays (Fig. 4). The energy released in (5) and (6) as quanta of electromagnetic radiation (γ) is absorbed by the liquid scintillator in the detector and reemitted at (near-)visible frequencies, which the PMTs can register. Energy and momentum conservation implies that the positron carries essentially all of the incoming antineutrino energy. The brightness of the prompt signal, as seen by the PMTs, scales with the positron kinetic energy. Thus the antineutrino energy can be determined for each IBD interaction. After collecting a number of events, the measured antineutrino spectrum is analyzed using elaborate data processing and statistical approaches, and deconvolved into geoneutrino signal and background (reactor antineutrino background and other backgrounds) (Gando et al., 2013; Agostini et al., 2020).

Geoneutrino Measurements

To date, two experiments have reported measurement of geoneutrinos: *KamLAND* (Kamioka, Gifu prefecture, Japan; first report 2010 and updates in 2011, 2013, 2016, 2019) and *Borexino* (Laboratori Nazionali del Gran Sasso, Italy; first report in 2010, updates in 2013, 2015, 2019). The evolution of the geoneutrino measurements is summarized in Table 2 and plotted in Fig. 5. For both experiments, the uncertainty of the measurement decreases with each measurement report, and all the measurements are consistent within uncertainty. The uncertainty is reduced with increasing exposure (more events, therefore decreased statistical uncertainty) and due to careful work by both experimental teams to reduce the systematic uncertainty (mostly by purifying the liquid scintillator and other components of the assembly, thus removing the non-antineutrino background). In the case of KamLAND experiment, additional systematic uncertainty reduction came with the shutdown of Japanese nuclear power stations after the Fukushima Daiichi nuclear disaster following the March 11, 2011 Tōhoku earthquake and tsunami (step decrease in reactor antineutrino background). There is a limit to decreasing the measurement uncertainty, even for a very long exposure, given by the systematics of each experiment (see Table 3).

Several other neutrino experiments are expected to measure geoneutrinos in the coming years (Table 3 and Fig. 3): *SNO+* (Sudbury, Ontario, Canada; Andringa et al., 2016) is currently being filled with scintillator, *JUNO* (Jiangmen, Guangdong province, China; An et al., 2016) is under construction with data taking expected to start in 2022, *JNE* (Jinping Mountains, Sichuan province, China; Beacom et al., 2017) is developing a 0.1-kton scale detector for testing purposes, *ANDES* is proposed at the planned Agua Negra Tunnel below the Andes mountains, connecting Chile and Argentina (Dib, 2015), and *BLVST* is proposed at the Baksan Neutrino Observatory in Russia (Petkov et al., 2020). Aside from these land-based experiments sitting in (or, at best, at the margin

Table 2 Geoneutrino measurements, as reported.

	Live-time (days)	Exposure (10^{32} p a)	Events (n)	Flux ($\text{cm}^{-2} \mu\text{s}^{-1}$)	Signal (TNU)
<i>KamLAND</i>					
Araki et al. (2005)	749	0.71	$28.0^{+15.6}_{-14.6}$		* 57 ± 31
Gando et al. (2011)	2135	3.49	106^{+29}_{-28}		* 38 ± 10
Gando et al. (2013)	2991	4.90	116^{+28}_{-27}	3.4 ± 0.8	* 30 ± 7
Watanabe (2016)	3901	6.39	164^{+28}_{-25}	$3.9^{+0.7}_{-0.6}$	$34.9^{+6.0}_{-5.4}$
Watanabe (2019)	4397	7.20	$168.8^{+26.3}_{-26.5}$	3.6 ± 0.6	32.1 ± 5.0
<i>Borexino</i>					
Bellini et al. (2010)	537.2		$9.9^{+4.1}_{-3.4}$		* 65^{+27}_{-22}
Bellini et al. (2013a)	1352.60	0.369 ± 0.016	14.3 ± 4.4		38.8 ± 12.0
Agostini et al. (2015)	2055.9	0.55 ± 0.03	$23.7^{+6.6}_{-5.7}$		$43.5^{+11.8}_{-10.4}(\text{stat})^{+2.7}_{-2.4}(\text{sys}) = 43.5^{+12.1}_{-10.7}$
Agostini et al. (2020)	3262.74	1.29 ± 0.05	$52.6^{+9.6}_{-9.0}$		$47.0^{+18.3\%}_{-17.2\%} = 47.0^{+8.6}_{-8.1}$

Recalculation to TNU performed where not provided in the original publication (indicated by * asterisk).

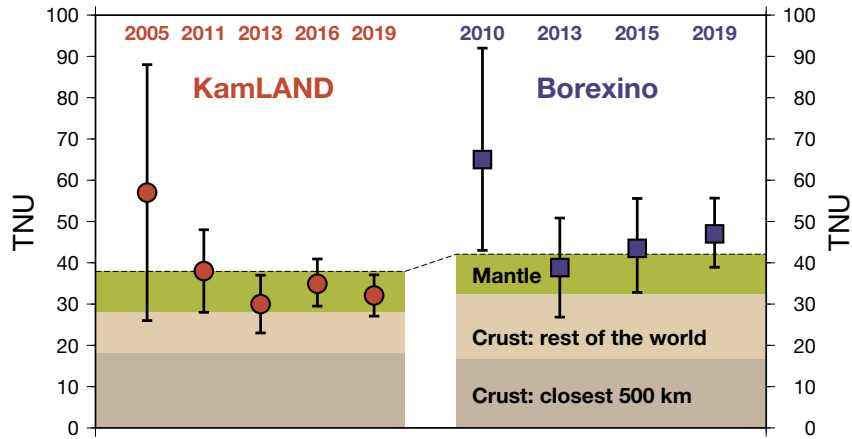


Fig. 5 Geoneutrino measurements and their uncertainty over time as reported by KamLAND (left, red) and Borexino (right, blue) experiments. The predicted signal of an Earth model with 20 TW of radiogenic power highlights contributions from the crust (shades of brown) and the mantle (green); see Wipperfurth et al. (2020) for details of the model.

Table 3 Geoneutrino detectors.

Detector	Location	Latitude ($^{\circ}$ N)	Longitude ($^{\circ}$ E)	Size (kton)	Depth (km.w.e.)	Meas. uncert.
KamLAND	Kamioka, Japan	36.43	137.31	0.9	2.7	16%
Borexino	LNGS, Gran Sasso, Italy	42.45	13.57	0.3	3.8	17%
SNO+	SNOLAB, Sudbury, Ontario, Canada	46.47	-81.20	0.8	5.4	9%
JUNO	Jiangmen, Guangdong, China	22.12	112.52	20	1.5	6%
JNE	Jinping, Sichuan, China	28.15	101.71	4	7.5	4%
BLVST	BNO, Caucasus, Russia	43.28	42.69	10	4.8	
ANDES	Agua Negra Tunnel, Chile/Argentina	-30.19	-69.82	3	4.5	5%
Hanohano/OBD	Oceans			10-50	~5	10%

Size in kilotons, depth in km water equivalent (km.w.e.).

Measurement uncertainty (last column) for future detectors is adopted from the relevant publications or estimated, based on statistical uncertainty, see Šrámek O, Roskovec B, Wipperfurth SA, Xi Y, and McDonough WF (2016) Revealing the Earth’s mantle from the tallest mountains using the Jinping Neutrino Experiment. *Scientific Reports* 6: 33034. <https://doi.org/10.1038/srep33034>.

of) continental crust, an ocean-going geoneutrino experiment *Hanohano/OBD* has long been proposed (Dye et al., 2006; Learned et al., 2008, further discussed in section *Prospects in geoneutrino research*).

Advancing Geoscience with Geoneutrinos

The ideas of using neutrinos for geophysics and astronomy go back to the years of the first neutrino detection efforts, as recorded by the exchange between G. Gamow and F. Reines (see, e.g., Fiorentini et al., 2007), and have been developed since then (Marx and Menyhard, 1960; Eder, 1966; Marx, 1969; Marx and Lux, 1970; Hamza and Beck, 1972; Avilez et al., 1981; Krauss et al., 1984; Kobayashi and Fukao, 1991; Raghavan et al., 1998; Rothschild et al., 1998; Raghavan, 2002; Mantovani et al., 2004; Enomoto, 2005).

Geoneutrino measurements enrich a geologist’s toolbox by providing, in principle, a gauge for the amount of geoneutrino emitters in the Earth (i.e., ^{40}K , ^{87}Rb , ^{232}Th , ^{238}U), therefore a reading of K, Rb, Th, U abundances, and consequently constraints on the abundances of other elements with similar geochemical behaviors. Ideally, a geoscientist would like to be able to detect the flux spectrum of geoneutrinos, both neutrinos and antineutrinos, emitted in decays of all the major radionuclides, and to determine their incoming direction and distance to emission point, in order to setup an *inverse problem* of mapping the concentrations and spatial arrangements of geoneutrino emitters in the Earth’s volume.

As is often the case, the imperfect world brings challenges: the currently deployed IBD technology only permits the detection of the highest energy antineutrinos of the ^{232}Th and ^{238}U decay chains (see next section); current detectors cannot determine the incoming direction (see next section); distance to emission point cannot be determined (this likely will never change, barring a paradigm shift in neutrino physics). Consequently, a geology-independent 3D mapping of radionuclides in the Earth based solely on geoneutrino measurements is not possible; geoscience-informed Earth models must be used to interpret the measurements.

The question one typically asks geoneutrinos to help resolve is: *How much Th and U are there in the Earth?* This relates to the longstanding debate about the composition of the Earth and the amount of radiogenic power available to drive Earth’s dynamics. Various estimates of the planet’s composition argue for present-day radiogenic heat production anywhere in the range of ~ 10 – 30 TW where Th and U together account for $\sim 80\%$ of the power, the remaining 20% is due to K. Given the insignificant amount of Th and U inferred in the Earth’s core (e.g., McDonough, 2016; Wipperfurth et al., 2018), and given geological (in the broad sense) models of Earth’s crustal structure and composition, the above question asked of geoneutrinos translates into: *How much Th and U is there in the Earth’s mantle?*

Useful answers to this question have begun to emerge. The first measurement by KamLAND carried a relative uncertainty of 55% (1σ). It was an exciting statement of the first detection of geoneutrinos. However, the result was compatible with all reasonable geological models of Earth’s composition, also with a fully radiogenic Earth model (where all of the present-day surface heat flow is due to radiogenic heat production, leaving no space for secular cooling of the planet). The uncertainty of the latest results dropped below 20% (16% for KamLAND and 18% for Borexino; Fig. 5), and geoneutrino measurements have now begun to discriminate between different proposed models of Earth’s chemistry (Fig. 6). Geoneutrino measurements also provide limits on a natural

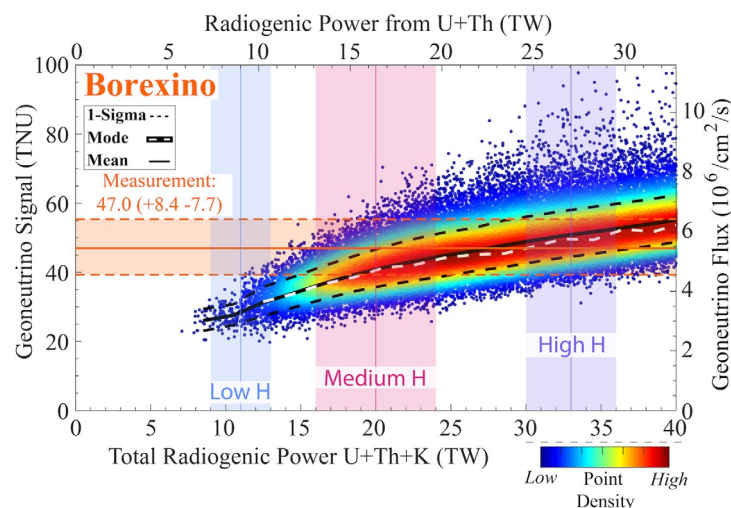


Fig. 6 Tradeoffs in linking the geoneutrino signal (vertical axes) to the amount of heat producing elements (expressed as radiogenic power; horizontal axes), shown for the Borexino site. The array of density-colored points is generated by Monte Carlo modeling based on an Earth compositional model, as done by Wipperfurth et al. (2020). Accounting for the uncertainties in the model, a given amount of Th + U distributed in the Earth can result in a range of predicted geoneutrino fluxes. Vice versa, a given (e.g., measured) value of geoneutrino flux is compatible with a rather broad range of Th + U concentrations. Figure from McDonough WF, Šramek O, and Wipperfurth SA (2020) Radiogenic power and geoneutrino luminosity of the Earth and other terrestrial bodies through time. *Geochemistry, Geophysics, Geosystems*, e2019GC008865. <https://doi.org/10.1029/2019GC008865>. arXiv:1912.04655; <https://doi.org/10.1002/essoar.10501374.1>.

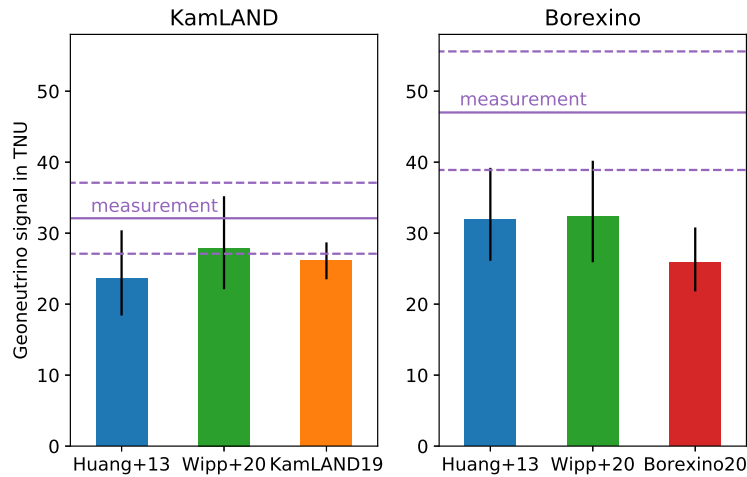


Fig. 7 Geoneutrino measurements and their uncertainties (purple lines) compared to crustal predictions of several models (bars): Huang et al. (2013) (blue), Wipperfurth et al. (2020) (green), Watanabe (2019) (orange, labeled as KamLAND19), Agostini et al. (2020) (red, labeled as Borexino20). The inferred mantle signal is the difference between the total measurement and the crustal prediction, and varies with one choice of the crustal model, for both KamLAND and Borexino.

georeactor, hypothesized by some to be currently operating at the center of the Earth: a georeactor with power ≥ 2.4 TW is excluded at 95% confidence level (Agostini et al., 2020).

However, challenges remain. To infer the mantle geoneutrino signal, a prediction of a signal from the crust, calculated using a geological crustal model, is subtracted from the total measured signal. Geoneutrino measurement comes with an uncertainty as discussed in section *Geoneutrino measurements* (Fig. 5). A geological model of Earth’s crust carries an uncertainty as well; furthermore, there is variation, sometimes significant, in crustal models constructed using different methods and by different research groups, as shown in Fig. 7. Predictions at continental sites (all of the current operating and constructed experiments) show a strong crustal geoneutrino signal (70–80% of the total), which is rather sensitive to the details of the nearby crust (closest few hundred km). As a result, at a continental measurement site, the inference of geoneutrino signal originating in the mantle carries a rather large uncertainty, which translates into comparably large uncertainty on the inferred radiogenic power in the Earth. Fig. 6 illustrates the situation for the Borexino setting.

The IBD-measured geoneutrino flux is a combination of signal from both ^{232}Th and ^{238}U decay chains. Given the distinct shape of antineutrino spectra from these two decay chains (Fig. 2), limits on Th/U ratio can be inferred from geoneutrino measurements (Watanabe, 2019). However, at present these are much looser than geochemical constraints (Wipperfurth et al., 2018, and references therein).

Prospects in Geoneutrino Research

The field of neutrino geoscience is young and evolving. Several directions of future developments have been outlined and are discussed in the following paragraphs.

It remains challenging to infer the mantle radiogenic power from geoneutrino measurements at continental experimental sites, where the signal is dominated by geoneutrinos emitted within the crust. It has been recognized that the best reading of the mantle signal can be obtained in an oceanic setting, far away from continents, where crustal signal is relatively small ($\leq 30\%$ of the total, due to thinner and less enriched oceanic crust) and nuclear reactors are distant (Dye et al., 2006) (see Fig. 8). A movable, ocean-going detector nicknamed Hanohano was proposed by a neutrino research group at the University of Hawaii (Learned et al., 2008), where the efforts included detailed engineering design based on currently available technologies (Makai Ocean Engineering, 2006); however, funding for the project has not been secured. The idea of an ocean-bottom detector (OBD) has recently been revived by a joint working group at JAMSTEC (Japan Agency for Marine-Earth Science and Technology) and Tohoku University (Japan). A precise reading of the mantle radiogenic power would resolve the longstanding debate about the energetics of mantle convection; specifically it would set the value of the *MANTLE UREY RATIO* (the ratio of radiogenic power in the mantle to the heat flux out of the mantle). Moreover, it is argued (Šrámek et al., 2013; Roskovec et al., 2020) that with an OBD, one could interrogate 3D structure of the Earth’s mantle and address fundamental geophysical questions about the mantle architecture such as “*Is the Earth’s mantle chemically uniform or more complex?*” and “*Are there large-scale geochemical anomalies in the shallow and/or the deep mantle?*”.

Another potential method to distinguish between crustal and mantle geoneutrino signal—one that could work at a continental detector location and does not require an oceanic measurement site—relies on the ability to determine the direction of the incoming geoneutrino. It is rather obvious geometrically that most of the crustal geoneutrinos arrive at a detector near the

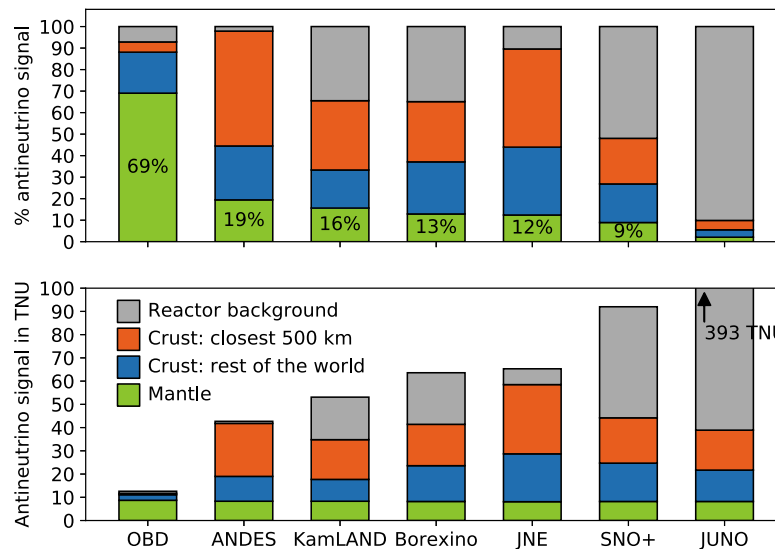


Fig. 8 Contributions to the total expected antineutrino signal (geoneutrinos and reactor antineutrinos) at the current and planned geoneutrino measuring experiments, ordered by the magnitude of the antineutrino signal. Note the large mantle contribution to the total signal at the oceanic detector (OBD). Based on the model by Šrámek O, Roskovec B, Wipperfurth SA, Xi Y, and McDonough WF (2016) Revealing the Earth's mantle from the tallest mountains using the Jinping Neutrino Experiment. *Scientific Reports* 6: 33034. <https://doi.org/10.1038/srep33034>.

horizontal direction (nadir angle near 90 degrees), while mantle geoneutrinos would show a broad angular distribution peaking at a moderate nadir angle; this was quantitatively confirmed by modeling (e.g., Dye, 2010). Current technology is not sensitive to the incoming direction of individual geoneutrinos. However, several ideas for a directional geoneutrino detector have been explored and are subject of ongoing research and development efforts (Tanaka and Watanabe, 2014; Leyton et al., 2017).

Current antineutrino detectors are sensitive to the highest energy geoneutrinos from ^{232}Th and ^{238}U decay chains. The entire spectrum of antineutrinos from ^{40}K decay lies below the IBD reaction energy threshold (Fig. 2). However, a measurement of ^{40}K geoneutrinos is desirable, as it would constrain the amount of K in the Earth, thus the K/U ratio of the volatile potassium to refractory uranium. This geochemistry-independent, particle physics measurement would help set the slope of the volatility curve for the planet (e.g., Bellini et al., 2013b). Research and experimental developments toward ^{40}K geoneutrino detection are advancing. While some envisage the inverse beta decay on a nucleus heavier than ^1H (a single proton) to lower the IBD threshold (Serafini, 2019), others propose to exploit, threshold-less interaction of neutrino–electron elastic scattering (Leyton et al., 2017; Wang and Chen, 2020).

Acknowledgment

The author is thankful to editor Ricardo Arevalo, Jr., and to colleagues Fabio Mantovani, William F. McDonough, Bedřich Roskovec, and Laura Sammon for many suggestions and critical reading of this chapter. Support for this work was provided by Czech Science Foundation grant GA17-01464S. Plots were made using Pyplot and Generic Mapping Tools with Scientific Color Maps.

References

- Agostini M, et al. and Borexino Collaboration (2015) Spectroscopy of geoneutrinos from 2056 days of Borexino data. *Physical Review D* 92: 031101. <https://doi.org/10.1103/PhysRevD.92.031101>. arXiv:1506.04610.
- Agostini M, et al. and Borexino Collaboration (2020) Comprehensive geoneutrino analysis with Borexino. *Physical Review D* 101: 012009. <https://doi.org/10.1103/PhysRevD.101.012009>. arXiv:1909.02257.
- An F, et al. (2016) Neutrino physics with JUNO. *Journal of Physics G* 43: 030401. <https://doi.org/10.1088/0954-3899/43/3/030401>. arXiv:1507.05613.
- Andringa S, et al. (2016) Current status and future prospects of the SNO+ experiment. *Adv. High Energy Phys.* 2016. <https://doi.org/10.1155/2016/6194250>.
- Araki T, et al. (2005) Experimental investigation of geologically produced antineutrinos with KamLAND. *Nature* 436: 499–503. <https://doi.org/10.1038/nature03980>.
- Arevalo R Jr., McDonough WF, and Luong M (2009) The K/U ratio of the silicate Earth: Insights into mantle composition, structure and thermal evolution. *Earth and Planetary Science Letters* 278: 361–369. <https://doi.org/10.1016/j.epsl.2008.12.023>.
- Avilez C, Marx G, and Fuentes B (1981) Earth as a source of antineutrinos. *Physical Review D* 23: 1116–1117. <https://doi.org/10.1103/PhysRevD.23.1116>.
- Baldoncini M, et al. (2015) Reference worldwide model for antineutrinos from reactors. *Physical Review D* 91: 065002. <https://doi.org/10.1103/PhysRevD.91.065002>.
- Beacom JF, et al. (2017) Physics prospects of the Jinping neutrino experiment. *Chinese Physics C* 41: 23002. <https://doi.org/10.1088/1674-1137/41/2/023002>.
- Bellini G, et al. and Borexino Collaboration (2010) Observation of geo-neutrinos. *Physics Letters B* 687: 299–304. <https://doi.org/10.1016/j.physletb.2010.03.051>.

- Bellini G, et al. and Borexino Collaboration (2013a) Measurement of geo-neutrinos from 1353 days of Borexino. *Physics Letters B* 722: 295–300. <https://doi.org/10.1016/j.physletb.2013.04.030>. arXiv:1303.2571.
- Bellini G, Ianni A, Ludhova L, Mantovani F, and McDonough WF (2013b) Geo-neutrinos. *Progress in Particle and Nuclear Physics* 73: 1–34. <https://doi.org/10.1016/j.pnpnp.2013.07.001>. arXiv:1310.3732.
- Close F (2010) *Neutrino*. Oxford University Press.
- Cowan GL, Reines F, Harrison FB, Kruse HW, and McGuire AD (1956) Detection of the free neutrino: A confirmation. *Science* 124: 103–104. <https://doi.org/10.1126/science.124.3212.103>.
- Dib CO (2015) ANDES: An underground laboratory in South America. *Physics Procedia* 61: 534–541. <https://doi.org/10.1016/j.phpro.2014.12.118>.
- Dye ST (2010) Geo-neutrinos and silicate earth enrichment of U and Th. *Earth and Planetary Science Letters* 297: 1–9. <https://doi.org/10.1016/j.epsl.2010.06.012>.
- Dye ST (2012) Geoneutrinos and the radioactive power of the Earth. *Reviews of Geophysics* 50, RG3007. <https://doi.org/10.1029/2012RG000400>. arXiv:1111.6099.
- Dye S, et al. (2006) Earth radioactivity measurements with a deep ocean anti-neutrino observatory. *Earth, Moon, and Planets* 99: 241–252. <https://doi.org/10.1007/s11038-006-9129-z>.
- Eder G (1966) Terrestrial neutrinos. *Nuclear Physics* 78: 657–662. [https://doi.org/10.1016/0029-5582\(66\)90903-5](https://doi.org/10.1016/0029-5582(66)90903-5).
- Enomoto S (2005) *Neutrino Geophysics and Observation of Geo-Neutrinos at KamLAND*. Ph.D. thesis. Tohoku University. Available from <http://kamland.lbl.gov/research-projects/kamland/student-dissertations/EnomotoSanhiro-DoctorThesis.pdf>
- Fiorentini G, Lissia M, Mantovani F, and Vannucci R (2005) Geo-neutrinos: A new probe of Earth's interior. *Earth and Planetary Science Letters* 238: 235–247. <https://doi.org/10.1016/j.epsl.2005.06.061>.
- Fiorentini G, Lissia M, and Mantovani F (2007) Geo-neutrinos and earth's interior. *Physics Reports* 453: 117–172. <https://doi.org/10.1016/j.physrep.2007.09.001>.
- Gando A, et al. and KamLAND Collaboration (2011) Partial radiogenic heat model for Earth revealed by geoneutrino measurements. *Nature Geoscience* 4: 647–651. <https://doi.org/10.1038/ngeo1205>.
- Gando A, et al. and KamLAND Collaboration (2013) Reactor on-off antineutrino measurement with KamLAND. *Physical Review D* 88: 033001. <https://doi.org/10.1103/PhysRevD.88.033001>. arXiv:1303.4667.
- Hamza VM and Beck AE (1972) Terrestrial heat flow, the neutrino problem, and a possible energy source in the core. *Nature* 240: 343–344. <https://doi.org/10.1038/240343a0>.
- Holden NE, Bonardi ML, De Bièvre P, Renne PR, and Villa IM (2011) IUPAC-IUGS common definition and convention on the use of the year as a derived unit of time (IUPAC Recommendations 2011). *Pure and Applied Chemistry* 83: 1159. <https://doi.org/10.1351/PAC-REC-09-01-22>.
- Huang Y, Chubakov V, Mantovani F, Rudnick RL, and McDonough WF (2013) A reference Earth model for the heat-producing elements and associated geoneutrino flux. *Geochemistry, Geophysics, Geosystems* 14: 2003–2029. <https://doi.org/10.1002/ggge.20129>. arXiv:1301.0365.
- Kobayashi M and Fukao Y (1991) The Earth as an antineutrino star. *Geophysical Research Letters* 18: 633–636. <https://doi.org/10.1029/91GL00800>.
- Krauss LM, Glashow SL, and Schramm DN (1984) Antineutrino astronomy and geophysics. *Nature* 310: 191–198. <https://doi.org/10.1038/310191a0>.
- Learned JG, Dye ST, and Pakvasa S (2008) Hanohano: A deep ocean anti-neutrino detector for unique neutrino physics and geophysics studies. *High Energy Physics – Experiment*. arXiv:0810.4975.
- Leyton M, Dye S, and Monroe J (2017) Exploring the hidden interior of the Earth with directional neutrino measurements. *Nature Communications* 8: 15989. <https://doi.org/10.1038/ncomms15989>. arXiv:1710.06724.
- Magill J and Galy J (2005) *Radioactivity Radionuclides Radiation*. Berlin Heidelberg: Springer-Verlag. <https://doi.org/10.1007/b138236>.
- Makai Ocean Engineering (2006) A Deep Ocean Anti-Neutrino Detector near Hawaii—Hanohano, Final Report. Prepared for: The National Defense Center of Excellence for Research in Ocean Sciences (CEROS). Prepared by: Makai Ocean Engineering, Inc. and Department of Physics and Astronomy, University of Hawaii, Manoa.
- Mantovani F, Carnignani L, Fiorentini G, and Lissia M (2004) Antineutrinos from Earth: A reference model and its uncertainties. *Physical Review D* 69: 013001. <https://doi.org/10.1103/PhysRevD.69.013001>.
- Marx G (1969) Geophysics by neutrinos. *Czechoslovak Journal of Physics B* 19: 1471–1479. <https://doi.org/10.1007/BF01698889>.
- Marx G and Lux I (1970) Hunting for soft antineutrinos. *Acta Physiologica Academiae Scientiarum Hungaricae* 28: 63–70. <https://doi.org/10.1007/BF03055146>.
- Marx G, and Menyhárd N (1960) Über die Perspektiven der neutrinoastronomie. *Mitteilungen der Sternwarte der Ungarischen Akademie der Wissenschaften Budapest-Szabadsághegy* 4.
- McDonough WF (2016) The composition of the lower mantle and core. In: Terasaki H and Fischer RA (eds.) *Deep Earth: Physics and Chemistry of the Lower Mantle and Core. Volume 217 of Geophysical Monograph Series*. 143–159. AGU and John Wiley & Sons, Inc. <https://doi.org/10.1002/9781118992487.ch12>.
- McDonough WF and Sun S (1995) The composition of the Earth. *Chemical Geology* 120: 223–253. [https://doi.org/10.1016/0009-2541\(94\)00140-4](https://doi.org/10.1016/0009-2541(94)00140-4).
- McDonough WF, Šrámek O, and Wipperfurth SA (2020) Radiogenic power and geoneutrino luminosity of the Earth and other terrestrial bodies through time. *Geochemistry, Geophysics, Geosystems*. e2019GC008865. <https://doi.org/10.1029/2019GC008865>. arXiv:1912.04655.
- Petkov VB, et al. (2020) Baksan large volume scintillation telescope: a current status. *Journal of Physics Conference Series* 1468: 012244. <https://doi.org/10.1088/1742-6596/1468/1/012244>.
- Raghavan RS (2002) Detecting a nuclear fission reactor at the center of the Earth. Available from <https://arxiv.org/abs/hep-ex/0208038>
- Raghavan RS, Schoenert S, Enomoto S, Shirai J, Suekane F, and Suzuki A (1998) Measuring the global radioactivity in the Earth by multidetector antineutrino spectroscopy. *Physical Review Letters* 80: 635–638. <https://doi.org/10.1103/PhysRevLett.80.635>.
- Roskovec B, Šrámek O, and McDonough WF (2020) Quantifying geochemical anomalies in the mantle using geoneutrinos. In: *Preparation (Previous Version on arXiv:1810.10914)*.
- Rothschild CG, Chen MC, and Calaprice FP (1998) Antineutrino geophysics with liquid scintillator detectors. *Geophysical Research Letters* 25: 1083–1086. <https://doi.org/10.1029/98GL50667>.
- Serafini A (2019) Detecting ^{40}K geoneutrinos with LiquidO. In: *Presentation at Neutrino Geoscience 2019 Prague, Czech Republic, October 21–23*. Available from <https://indico.cern.ch/event/825708/contributions/3550280/>.
- Šrámek O, McDonough WF, Kite ES, Lekić V, Dye ST, and Zhong S (2013) Geophysical and geochemical constraints on geoneutrino fluxes from Earth's mantle. *Earth and Planetary Science Letters* 361: 356–366. <https://doi.org/10.1016/j.epsl.2012.11.001>. arXiv:1207.0853.
- Tanaka HKM and Watanabe H (2014) ^6Li -loaded directionally sensitive anti-neutrino detector for possible geo-neutrino-graphic imaging applications. *Scientific Reports* 4: 4708. <https://doi.org/10.1038/srep04708>.
- Usman SM, Jocher GR, Dye ST, McDonough WF, and Learned JG (2015) AGM2015: Antineutrino Global Map 2015. *Scientific Reports* 5: 13945. <https://doi.org/10.1038/srep13945>.
- Vitagliano E, Tamborra I, and Raffelt G (2019) Grand unified neutrino spectrum at Earth. arXiv: 1910.11878.
- Vogel P and Beacom JF (1999) Angular distribution of neutron inverse beta decay, $\bar{\nu}_e + p \rightarrow e^+ + n$. *Physical Review D* 60: 053003. <https://doi.org/10.1103/PhysRevD.60.053003>.
- Wang Z and Chen S (2020) Hunting potassium geoneutrinos with liquid scintillator Cherenkov neutrino detectors. *Chinese Physics C* 44: 033001. <https://doi.org/10.1088/1674-1137/44/3/033001>. arXiv:1709.03743.
- Watanabe H (2016) KamLAND. In: *International Workshop: Neutrino Research and Thermal Evolution of the Earth, Tohoku University, Sendai, October 25–27*. Available from http://www.tfc.tohoku.ac.jp/wp-content/uploads/2016/10/04_HirokoWatanabe_TFC2016.pdf.
- Watanabe H (2019) Geo-neutrino measurement with KamLAND. In: *Presentation at Neutrino Geoscience 2019 Prague, Czech Republic, October 21–23*. Available from <https://indico.cern.ch/event/825708/contributions/3552210/>.
- Wipperfurth SA, Guo M, Šrámek O, and McDonough WF (2018) Earth's chondritic Th/U: Negligible fractionation during accretion, core formation, and crust–mantle differentiation. *Earth and Planetary Science Letters* 498: 196–202. <https://doi.org/10.1016/j.epsl.2018.06.029>. arXiv:1801.05473.
- Wipperfurth SA, Šrámek O, and McDonough WF (2020) Reference models for lithospheric geoneutrino signal. *Journal of Geophysical Research* 125: e2019JB018433. <https://doi.org/10.1029/2019JB018433>. arXiv:1907.12184.

Relevant Websites

<https://www.awa.tohoku.ac.jp/kamland/>—KamLAND.

<http://borex.lngs.infn.it/>—Borexino.

<http://snoplus.phy.queensu.ca/>—SNO+.

<http://juno.ihep.cas.cn/>—JUNO.

<http://jinping.hep.tsinghua.edu.cn/>—JNE.

<http://andeslab.org/>—ANDES.

<https://geoneutrinos.org/>—Interactive plotting of geoneutrino and reactor antineutrino flux.

<https://indico.cern.ch/e/ngs2019/>—The last edition of the Neutrino Geoscience conference.

<http://geo.mff.cuni.cz/~sramek/research/geonuEncGeo12/>—Some calculations and Pyplot figures prepared for this chapter are available as Jupyter Notebook.